RAPID COMMUNICATIONS

PHYSICAL REVIEW B VOLUME 46, NUMBER 3 15 JULY 1992-I

Connecting carbon tubules

B. I. Dunlap

Theoretical Chemistry Section, Code 6179, Naval Research Laboratory, Washington, D.C. 20375-5000

(Received 25 February 1992; revised manuscript received 13 April 1992)

Two possible joints between different types of carbon tubules are discussed. Both joints introduce a single pentagon-heptagon pair into the perfect hexagon bonding pattern of the two tubules. These two types of joints can be used to form composite tubules in which every carbon atom is threefold coordinated. The first type of joint removes or adds a single hexagon from the circumference of the tubule and the second joins specific "crenelated" and "sawtooth" tubules of significantly different radii at an angle of 30°.

There has been an explosive growth in the number of new all-carbon molecules following on the heels of the breakthrough of Krätschmer, Huffman, and coworkers,[1] which led to macroscopic amounts of C_{60} and C_{70} having icosahedral and D_{5h} symmetries, respectively. C_{76} has been isolated and found to be D_2 symmetric and thus chiral.[2] C_{78} has been isolated and found to be a mixture of two different isomers, one having C_{2v} symmetry and the other, less abundant, isomer having D_3 symmetry.[3] There is every reason to expect the number of different fullerenes produced in macroscopic amounts to continue to grow. It is hard to imagine limits on the different shapes that these molecules might assume. In particular, one need not assume all such molecules will be almost round nor that they will all be made using gas-aggregation methods. The existence of microscopic carbon tubules has been postulated theoretically[4] and discovered in electron microscopy of carbon electrodes.[5] A beam of electrons can apparently fuse fullerenes together.[6] One might be able to fuse tubules together in a similar fashion. In any event, the infinite and semi-infinite tubules are simple systems with which to begin a discussion of the fusion of all-carbon molecules.

Figure 1(a) shows a classification scheme for tubules. Joining any two vertices of a planar graphene sheet forms a tubule of circumference OM, which in turn can be decomposed into its components OL and LM along two conventional primitive translation directions of the graphene lattice. Additionally $L \geq M$ give the number of unit cells (containing two atoms) traversed in each direction. If M is zero, then a "zigzag"[4] or "sawtooth"[7] tubule is formed. If $L = M$, then an "armchair"[4] or "crenelated" tubule is formed. In all other cases the tubule is chiral (different from its mirror image). If a sawtooth tubule is cut in half normal to its axis, then the newly exposed edges have alternating raised and lowered carbons. The bonds connecting these terminal carbon atoms form a pattern that is reminiscent of the cutting edge of a hole-saw bit for an electric drill. If a crenelated tubule is cut normal to its axis, then the two edges are duller, being composed of alternately raised and lowered pairs of carbon atoms.

The crenelated tubules are potentially of great technological importance because they could become the basis of the first intrinsically conducting one-dimensional and organic polymers.[8] The band gaps of some sawtooth[9] and chiral[10] tubules have been computed, and the band gaps of all tubules have been estimated from the band structure of a graphene sheet.[9,11]

Several features of Fig. 1(a) are useful in discussing the joining of tubules. The line OM is the tubule circumference perpendicular to the tubule axis. The length of this circumference is

$$OM = a\sqrt{3(L^2 + M^2 + LM)}, \tag{1}$$

where a is the nearest-neighbor distance. The circumfer-

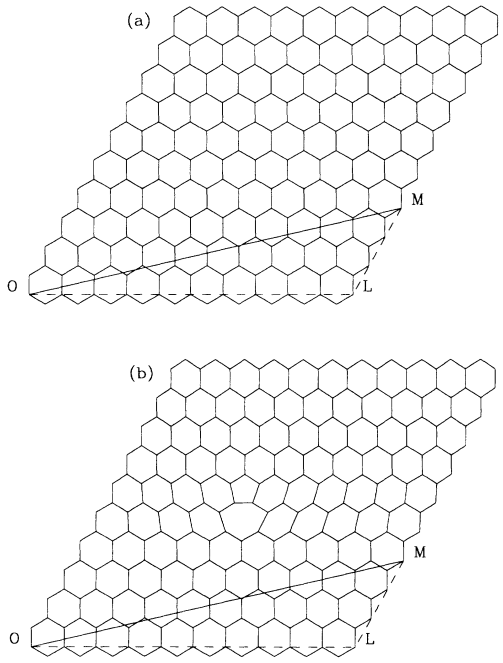

FIG. 1. The tubule labeling convention for perfect tubules (a) and its extension to imperfect tubules (b). The left edge of each figure is to be mated to the right edge so that the points O and M are superposed. In that case the line OM becomes a tubule circumference.

ence cuts $M + L$ carbon-carbon nearest-neighbor bonds. Thus two tubules having the same sum $M + L$ may, in principle, be joined together coaxially while still preserving the threefold coordination of each carbon atom. The problem of joining two tubules having the same $M + L$ together is that the circumferences differ—most dramatically between crenelated tubules (L, L) having circumference $3L$ and sawtooth tubules $(2L, 0)$ having circumference $2L\sqrt{3}$. For small enough tubules, however, (L, L) and $(2L, 0)$ tubules can be cut normal to their axes and joined together forming a ring of L abutting pentagon-heptagon pairs.

Figure 1(b) shows the topology of a simple defect in a graphene sheet that preserves threefold coordination of each carbon atom and introduces a long-range tubule change. In contrast to Fig. 1(a), L and M cannot be interchanged without getting a distinct tubule. All horizontal rows of polygons above the heptagon contain eleven polygons and all horizontal rows below the pentagon contain ten polygons. Clearly the left and right edges of the figure can be joined to form a tubule which is a splicing together of (L, M) and $(L+1, M)$ semi-infinite tubules. In this case there is only one abutting pentagon-heptagon pair introduced. Strain associated with this defect will be localized, and far enough away from it the half tubules will have circumferences given by Eq. (1). This defect will bend the two halves of the tubule unless $M = 0$.

If the heptagon-pentagon direction in Fig. 1(b) is rotated from pointing upward to pointing to the right, an extra half line of hexagons will occur on the right half of the figure. Wrapping the left and right edges together and distorting so that both edges can be zippered together will result in a tubule that has M decreased by one unit in going from bottom to top.

Thus heptagon-pentagon pairs can be used to continuously change the character of the tubule. For example, they could be used to taper the ends of a tubule. Iijima[5] has seen curved, polygonal, and cone-shaped tubule caps. The conic caps have specific opening angles, either 19° or 40°, which are the only opening angles possible if a graphene sheet is rolled into a cone with overlapping vertices. For a given opening-angle direction these two cones result from overlapping one vertical bond from Fig. 1(a) with each of the other two classes of nonvertical bonds. The only nonhexagonal polygons of a 40° cone, which is twofold about its axis, are a square connected to two pentagons at its apex and two pentagons at its mouth. Such a cone can only mate coaxially with a sawtooth tubule. The chiral tubules seen in electron microscopy[5] could be transformed into sawtooth tubules and mated smoothly and coaxially with a 40° conical cap by repeatedly using this defect. The adjacent heptagon-pentagon pair introduces a gentle tubule transformation.

A dramatic tubule transformation is the joining together of a crenelated and a sawtooth tubule of appropriate diameters. Two examples of this joint are shown in Fig. 2. If an (L, L) crenelated tubule is cut at a 30° angle with respect to the tube axis, then an edge is exposed that has a sawtooth bonding pattern between all edge carbon atoms except for two crenelated connections that appear in the top foreground and top background of the tubule drawn in the lower right part of both panels of Figs. 2(a) and 2(b). Thus the appropriate (L, L) sawtooth tubule drawn in the upper right of both parts of the figure mates perfectly except at those two points. The four atoms that touch at these two defects when these two tubules join are connected by lines in the exploded view. In the fused tubules, drawn to the left in parts

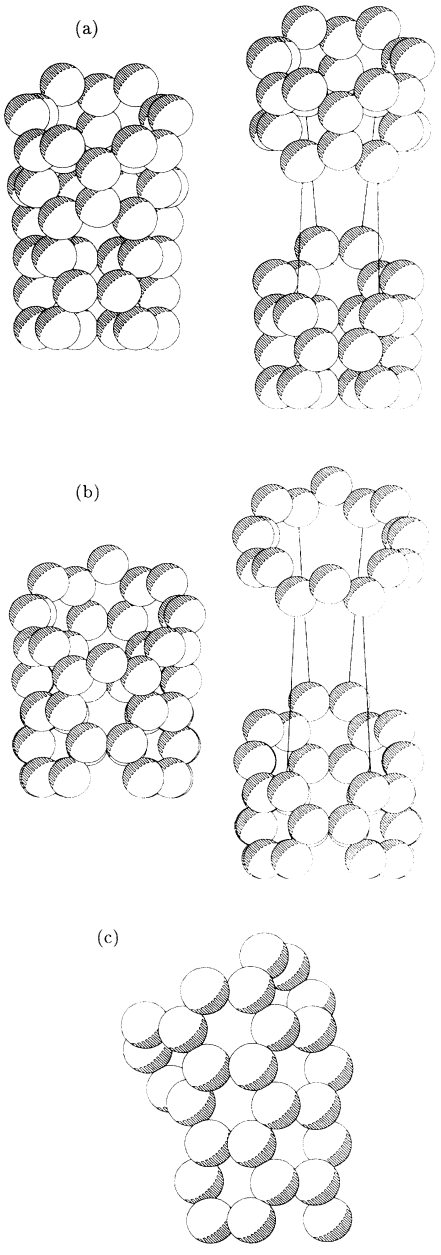

FIG. 2. The 30° joint between sawtooth tubules (top) and crenelated tubules (bottom) resulting in a single heptagonal defect (foreground) and a single pentagonal defect (background). A $(6, 0)$ sawtooth tubule and a $(3, 3)$ crenelated tubule connect in panel (a) and an $(8, 0)$ sawtooth tubule and a $(4, 4)$ crenelated tubule connect in panel (b). A side view of the joint between the smaller diameter tubules is shown (c). These atoms can also be reflected and translated twelve times to yield a C_{540} torus (a) and (c) and a C_{576} torus (b).

(a) and (b) of Fig. 2, these touching atoms are part of a heptagon that occurs in the foreground, in the crook of the elbow, or are part of a pentagon that occurs in the background, at the apex of the elbow. The pentagon is visible in Fig. 2(b), where the sawtooth tubule is represented by a single strand of carbon atoms. Again the strain associated with the pentagon and heptagon is localized. Figure 2(c) shows a side view of the connection between (6,0) and (3,3) tubules. This view, in which the heptagon and the pentagon are hidden, shows no strain other than the cylindrical curvature of the two tubules themselves. Close to this joint, already at the top and bottom of Fig. 2(c), the crenelated and sawtooth tubules are perfect yet have axes that meet at a 30° angle. The pentagon is associated with a curvature that has the same sense in both surface directions, as are the pentagons in the fullerenes.[12] The heptagon is associated with a saddle point on the surface, as are the heptagons in a negative curvature analog of C_{60}.[13]

Because this sawtooth-to-crenelated joint results in a 30° bend, twelve such joints can be repeated to form a closed toroidal molecule, the surface of which is covered by hexagons except for twelve heptagons and twelve pentagons. In fact, the atoms depicted in Figs. 2(a) and 2(b) are the symmetry inequivalent atoms of C_{6v} symmetric tori containing 540 and 576 atoms, respectively. The geometry of these tori have been optimized using an empirical potential[14] and the optimized positions displayed in the figure. There is very little apparent distortion from cylindrical shape for the tubule segments in this figure. Minimal distortion is also demonstrated in Table I, in which the tori empirical-potential binding energies per atom are shown to be bounded by the binding energy per atom of the two relevant infinite tubules.[7] These tori binding energies can also be compared to those of finite systems. The empirical-potential binding energies of icosahedral C_{60} and C_{240} are 7.044 and 7.269 eV per atom, respectively, which also bracket these tori binding energies.

Crenelated tubules are metals.[8] One might expect these tori that have roughly half of their atoms in crenelated configurations to have small highest occupied molecular orbital–lowest occupied molecular orbital (HOMO-LUMO) gaps. An all-valence tight-binding-model parametrization[7,15] reproduces the first-principles local-density-functional (LDF) band structure of a (5,5) tubule.[10] Figure 3 compares this tight-binding-model

TABLE I. Optimized empirical-potential binding energies (BE) in electron volts per carbon atom for the two tori of Fig. 2. Each tori binding energy is compared to the optimized empirical-potential energies per carbon atom for the two infinite tubules, the sections of which depicted in Fig. 2 join repeatedly to make the tori.

	BE (eV)	(L,M)	BE (eV)	(L,M)
Crenelated[a]	7.122	(3,3)	7.233	(4,4)
Torus	7.171		7.237	
Sawtooth[a]	7.181	(6,0)	7.267	(8,0)

[a] From Ref. 7.

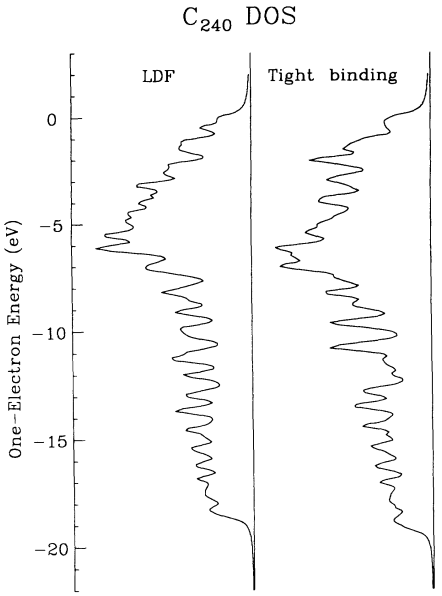

FIG. 3. Comparison of the all-valence tight-binding model (Ref. 6) and the local-density-functional (Ref. 11) density of states for C_{240}.

electronic density-of-states (DOS) Lorentzian broadened by 0.2 eV for C_{240} against the LDF DOS.[16] The width of the valence band, the position of the maximum, and the overall shape of the DOS in the two methods agree. The empirical potential and LDF HOMO-LUMO gaps for C_{240} are 1.0 and 1.2 eV, respectively. The empirical-potential HOMO-LUMO gaps for the 540- and 576-atom tori are 0.04 and 0.02 eV, respectively, substantially reduced from the HOMO-LUMO gaps of closed-shell fullerenes. There are also substantial differences between fullerene and toroidal valence-band DOS's. Comparing Fig. 4 to Fig. 3 shows that the tori have a large increase

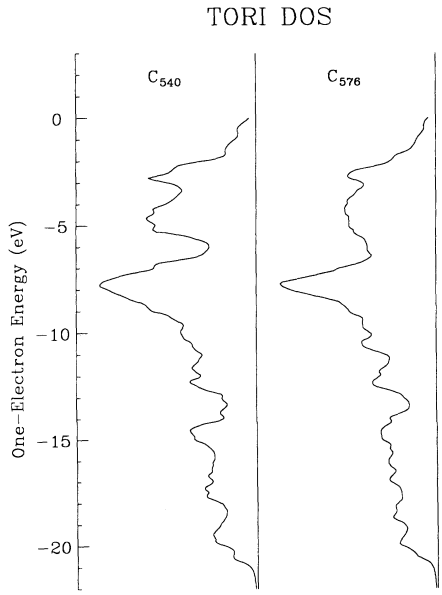

FIG. 4. Tight-binding model toroidal density of states.

in the density of states at the top of the valence band. The DOS region from -3 to -5 eV in these figures shows the greatest difference between the fullerene and the tori.

In conclusion, different carbon tubules can be connected together in an infinite number of ways. It is possible to connect two different tubules together using a single pentagon and a single heptagon at the joint. Two such connections, introducing small and large amounts of bending, have been described herein. The stability of these two joints is indicated by the fact that the empirical-potential binding energies of finite tori made using twelve such joints are bracketed by the binding energies of the two corresponding infinite tubules. These joints also fuse halves of appropriate, finite-sized fullerenes together.

Note added in proof. Tabule transformations by a single heptagon-pentagon pair have been seen in electron microscopy.[17]

I thank John Mintmire, Carter White, Don Brenner, Rick Mowrey, and Daniel Robertson for helpful discussions and technical help with these calculations. This work was supported in part by the Office of Naval Research through the Naval Research Laboratory.

[1]W. Krätschmer, L. D. Lamb, K. Fostiropolous, and D. R. Huffman, Nature **347**, 354 (1990).
[2]R. Ettl, I. Chao, F. Diederich, and R. L. Whetten, Nature **353**, 149 (1991).
[3]F. Diederich, R. L. Whetten, C. Thilgen, R. Ettl, I. Chao, and M. M. Alverez, Science **254**, 1768 (1991).
[4]M. S. Dresselhaus, G. Dresselhaus, and R. Saito, Phys. Rev. B **45**, 6234 (1992).
[5]S. Iijima, Nature **354**, 56 (1991).
[6]S. Wang and P. R. Buseck, Chem. Phys. Lett. **182**, 1 (1991).
[7]D. H. Robertson, D. W. Brenner, and J. W. Mintmire, Phys. Rev. B **45**, 12 592 (1992).
[8]J. W. Mintmire, B. I. Dunlap, and C. T. White, Phys. Rev. Lett. **68**, 632 (1992).
[9]N. Hamada, S. Sawada, and A. Oshiyama, Phys. Rev. Lett. **68**, 1579 (1992).
[10]J. W. Mintmire, D. H. Robertson, B. I. Dunlap, R. C. Mowrey, D. W. Brenner, and C. T. White, in *Electrical, Optical, and Magnetic Properties of Organic Solid State Materials*, edited by L. Y. Chiang, A. F. Garito, and D. J. Sandman, MRS Symposia Proceedings No. 247 (Materials Research Society, Pittsburgh, 1992), p. 339.
[11]R. Saito, M. Fujita, G. Dresselhaus, and M. S. Dresselhaus, in *Electrical, Optical, and Magnetic Properties of Organic Solid State Materials* (Ref. 10), p. 333.
[12]H. W. Kroto, A. W. Allaf, and S. P. Balm, Chem. Rev. **91**, 1213 (1991).
[13]D. Vanderbilt and J. Tersof, Phys. Rev. Lett. **68**, 511 (1992).
[14]D. W. Brenner, Phys. Rev. B **42**, 9458 (1990).
[15]C. T. White (unpublished).
[16]B. I. Dunlap, D. W. Brenner, J. W. Mintmire, R. C. Mowrey, and C. T. White, J. Phys. Chem. **95**, 8737 (1991).
[17]S. Iijma, T. Ichihashi, and Y. Ando, Nature **356**, 776 (1992).